Deep investigation of a pair of open clusters NGC 7031 and NGC 7086 utilizing Gaia DR3

A.A. Haroon[1,4] , **W.H. Elsanhoury**[2,4] , **A.S. Saad**[3,4] and

E.A. Elkholy[2,4]

[1] *Astronomy and Space Science Department, Faculty of Science, King Abdulaziz University, Jeddah, Saudi Arabia(E-mail: aaharoon@kau.edu.sa)*

[2] *Department of Physics, College of Science, Northern Border University, Arar, Saudi Arabia(E-mail: elsanhoury@nbu.edu.sa)*

[3] *Operations Management Department, College of Business and Economics, Qassim University, Buraidah 51452, Qassim, Saudi Arabia(E-mail: rmthaan@qu.edu.sa)*

[4] *Astronomy Department, National Research Institute of Astronomy and Geophysics (NRIAG), 11421, Helwan, Cairo, Egypt (E-mail: elsanhoury@nriag.sci.eg)*

Abstract. In this paper, we carried out photometric and kinematic study of two poorly studied open clusters NGC 7031 and NGC 7086 utilizing the optical wavelength of Gaia DR3. We identified 613 and 226 candidates for respective clusters as highly probable astrometric members. Fitting King's profile within RDPs, we estimate both core and limiting radii. For each cluster, we construct CMDs and fit them with suitable isochrones with metallicities (Z = 0.01189 $\pm$ 0.00023 & 0.01121 $\pm$ 0.00025) and different ages (8.468 $\pm$ 0.007 & 8.617 $\pm$ 0.021; log yr^{-1}), therefore, the heliocentric distances are 701 $\pm$ 26 & 942 $\pm$ 31 pc for NGC 7031 and NGC 7086, respectively. Moreover, the collective mass (M_C) in solar mass units may be deduced with MLR of 1072 $\pm$ 33 & 598 $\pm$ 25 and LF concluded that the average absolute (M_G) magnitudes are 7.51 $\pm$ 0.36 & 6.54 $\pm$ 0.39 for respective clusters. The overall mass function reflects the slopes (α) for Salpeter's value (2.35) within the uncertainty, i.e., $\alpha_{\text{NGC 7031}} = 2.73 \pm 0.25$ & $\alpha_{\text{NGC 7086}} = 2.67 \pm 0.32$.

The present study and the dynamical analysis for different evolving times demonstrate that the clusters are dynamically relaxed, where the dynamical evolution parameter $\tau \gg 1$. According to a kinematical analysis, we have obtained that the coherent convergent point (A_o, D_o) is (-83º.99 $\pm$ 0º.11, -24º.02 $\pm$ 0º.20; NGC 7031) & (-80º.69 $\pm$ 0º.11, -17º.51 $\pm$ 0º.24; NGC 7086). Finally, we have computed their linear separation distance to be about 55.08 $\pm$ 7.42 pc, which reflects that the clusters are not binary and/or pair clusters.

Key words: open clusters: NGC 7031 and 7086 – astrometric – color magnitude diagrams CMDs – photometric – kinematics

1. Introduction

Open star clusters (OCs) are uniform stellar systems with abundant gas and dust that originated along the Galactic plane under identical physical scenarios. They are found in varied ranges of stellar mass but contain tens to a few thousand stars spread across comparable distances, ages, and initial chemical compositions. As a result, each of these systems makes an excellent laboratory for researching the creation and evolution of stars, and it may be utilized to test and constrain theories regarding stellar evolution (Joshi et al., 2016). In addition to offering details on the physics, motion, and development of stars, OCs also show the Milky Way's disk structure (Kharchenko et al., 2013). Because of their ability to accurately determine the amount of interstellar reddening towards them, their chemical abundances, distances, and ages, OCs are a great tool for studying the structural, dynamic, and chemical evolution of the galaxy. This is demonstrated by the ability to create two-color diagrams (TCDs) and color-magnitude diagrams (CMDs) from UBV photometric data, and then compare these diagrams with stellar models and isochrones.

According to earlier studies, the percentage of OCs in gravitationally interacting pairs[1] is not insignificant in this situation (Angelo et al., 2022). At a distance of 50–60 kpc, the Magellanic Clouds (MCs) make it simple to identify binary clusters (Hatzidimitriou & Bhatia, 1990). It appears from studies of the Large Magellanic Cloud (LMC) and Small Magellanic Cloud (SMC) that about 10% of clusters are binary and/or pair clusters (Pietrzynski & Udalski, 2000) far from each other appearing to be close due to a viewing angle (Conrad et al., 2017). Some research (Subramaniam et al., 1995) has found that the Milky Way's binary cluster percent age is less than this (~ 8 %; 18 probable pairs) and stated that a cluster pair is termed a binary cluster if the separation is ≤ 20 pc.

Also, de La Fuente Marcos & de La Fuente Marcos (2009) used information from the Dias et al. (2002) and WEBDA[2] (Netopil et al., 2012) catalogs for a volume-limited sample of OCs that were situated at the solar circle. They used the physical (as opposed to projected) separation between pairs of OCs as their primary selection criterion, presuming that two objects are part of an interacting system when their separation is less than three times the average tidal radius (r_t) for clusters in the Milky Way disc $\sim$10 pc (Binney & Tremaine, 2008). Based on the results of their process, they concluded that, like what has been proposed for the Magellanic Clouds (e.g., Bhatia & Hatzidimitriou (1988); Hatzidimitriou & Bhatia (1990); Pietrzynski & Udalski (2000); Dieball et al. (2002)), at least ~ 10 % of all OCs seem to be involved in some kind of interaction with another cluster.

---

[1] The term "pairs" is used simply to describe either unbound or gravitationally bound groups of interacting OCs or even random alignments in the sky. The term "binary cluster" is specifically used to refer to clusters of two OCs that are gravitationally bonded.

[2] https://webda.physics.muni.cz/

Table 1. Astrophysical parameters of NGC 7031 and NGC 7086, which were derived from the literature; (1)Dias et al. (2002), (2)Svolopoulos (1961), (3)Hoag et al. (1961), (4)Lindoff (1968), (5)Hassan & Barbon (1973), (6)Kopchev & Petrov (2008), (7)Yontan et al. (2019), (8)Hassan (1967), (9)Rosvick & Robb (2006), (10)Hunt & Reffert (2024).

α_{2000} [h m s]	δ_{2000} [° ′ ″]	l [°]	b [°]	$E(B-V)$ [mag]	$m-M$ [mag]	Distance [pc]	$\log t$ [yr^{-1}]	d_{Gaia} [pc]	$\mu_\alpha^\star$ [mas yr^{-1}]	μ_δ [mas yr^{-1}]	Ref.
						Cluster: **NGC 7031**					
21 07 12.00	50 52 30	91.33	2.31	0.854	-	900	8.138	-	-2.87±0.20	-4.77±0.11	(1)
				1.03	12.60	760	-	-	-	-	(2)
21 08.20 0	50 42 0.0	91.62	2.04	0.85	12.41	900	8.14	-	-	-	(3)
				-	12.25	910	7.75	-	-	-	(4)
21 05.70 0.0	50 38 0.0	91.03	2.30	0.71-0.84	11.45-11.70	730-686	8.68	-	-	-	(5)
				1.05±0.05	9.60±0.20	831±72	8.35	-	-	-	(6)
				0.93±0.08	13.30±0.25	1212±146	7.81±0.03	1414±81	-1.286±0.081	-4.144±0.076	(7)
21 07 12.76	50 51 56.20	91.65	2.24	0.973	10.756	1416	7.562	-	-1.243±0.008	-4.281±0.010	(10)
						Cluster: **NGC 7086**					
21 30 27.0	51 36 0.0	94.41	0.22	0.807	-	1298	8.142	-	0.98±1.56	0.22±1.44	(1)
21 29.40 0	51 27 0.0	94.48	0.24	0.69	12.40	1170	8.87	-	-	-	(8)
				-	12.50	1205	7.93	-	-	-	(4)
21 30 30	51 36 0.0	94.40	0.20	0.83±0.02	13.40±0.30	1500	8.00	-	-	-	(9)
				0.75±0.05	9.90±0.20	955±84	8.25±0.06	-	-	-	(6)
				0.75±0.07	13.37±0.23	1618±182	8.18±0.07	1684±140	-1.642±0.086	-1.644±0.076	(7)
21 30 30.66	51 35 34.10	94.76	0.19	0.991	11.129	1681	8.183	-	-1.653±0.005	-1.664±0.004	(10)

In the present work, we carried out the extensive astrometric, photometric, and kinematic analysis of a poorly studied pair and/or binary clusters NGC 7031 (known as Collinder 430, FSR 294, MWSC 3466, NGC 7031, OCL 210, or Theia 2164) and NGC 7086 (known as Collinder 437, FSR 309, MWSC 3520, NGC 7086, OCL 214, or Theia 2737) open clusters (Hunt & Reffert, 2023), which are located very near to the disc of the Milky Way (MW) according to Gaia Mission Collaborations data release 3 Gaia Collaboration (2022). Table 1 presents the the fundamental and astrophysical parameters of NGC 7031 and NGC 7086, which are derived from the literature like Dias et al. (2002), Svolopoulos (1961), Hoag et al. (1961), Lindoff (1968), Hassan & Barbon (1973), Kopchev & Petrov (2008), Yontan et al. (2019), Hassan (1967), Rosvick & Robb (2006), and Hunt & Reffert (2024).

In what follows, Section 2 describes the Gaia DR3 data we used. The structural analysis of the OCs is given in Section 3 followed by the discussion and selection of the probable members to construct CMDs in Section 4 with various photometric parameters. Luminosity, mass functions, and mass segregation are described in Section 5. Section 6 deals with evolving times and escape velocity. The ellipsoidal motion and the kinematical structure are presented in Section 7. We close finally with conclusions in Section 8.

2. Data sample

In this study, we have extracted our target with the aid of the most recent Gaia mission collaborations data release 3 of Gaia Collaboration (2022) to get the astrometric data. A new era in astronomy began with the launch of the European Space Agency (ESA) mission Gaia as it contains the five-parameter astrometry for approximately 1.8 billion sources along their position in the sky (α, δ), parallaxes $(\pi; \text{mas})$ and the right ascension and declination components of the proper motion $(\mu_\alpha^\star, \mu_\delta; \text{mas yr}^{-1})$[3] with limiting magnitude of $G = 21$ mag. With uncertainties in the respective proper motion, components are up to $0.02 – 0.03$ mas yr^{-1} (at G < 15 mag), 0.07 mas yr^{-1} (at G ∼ 17 mag), 0.50 mas yr^{-1} (at G ∼ 20 mag) and 1.40 mas yr^{-1} (at G = 21). The uncertainties in the parallax values are ∼ $0.02 – 0.03$ mas for sources with G < 15 mag, ∼ 0.07 mas for sources with $G = 17$ mag, ∼ 0.50 mas at $G = 20$ mag, and ∼ 1.30 mas at $G = 21$. The DR3 is complemented with data of the radial velocity (V_r) for about 7 million stars from DR2 Gaia Collaboration et al. (2021). The source list has a slight change to DR2 with some notable changes. The significant advance of DR3 over DR2 is the large improvement in the accuracy of the astrometric parameters; a factor of 2.00 in the proper motion accuracy and a factor of about 1.50 in the parallax accuracy. Astrometric errors were suppressed by $30 – 40\%$ for the parallax and by a factor of 2.50 for the proper motion.

---

[3]$(\mu_\alpha^\star = \mu_\alpha \cos \delta)$

In our calculations, the downloaded data was taken from the Gaia DR3 catalog of Gaia Collaboration (2022). Although the apparent diameters of these two open clusters are about 14.0 and 12.0 arcmin, respectively, we need to download the data diameter of both by about 20 arcmin to reach the background field stars. Therefore, we get from the Gaia DR3 catalog a complete worksheet data including the angular distance from the center, right ascension, and declination for G mag for NGC 7031 and NGC 7086.

3. Structural analysis of the open clusters

The initial phase of analyzing a cluster involves determining its structural attributes, such as the central coordinates and the outermost boundary. Despite some catalogs providing this information, the accuracy of the listed centers and sizes is not always reliable. For the analysis of structural and essential characteristics in this research, we consistently employ the ASteCA software suite. This package has been utilized in the examination of numerous clusters in previous studies and has yielded outstanding outcomes, e.g. Perren et al. (2020).

3.1. Determination of the new center of the clusters

In contrast to globular clusters where the center is typically clear to the naked eye, the core of an OC might not be as easily discernible. The Automated Stellar Cluster Analysis (ASteCA) code of Perren et al. (2015) employs a widely used technique to ascertain an OC's central coordinates by identifying the point with the highest spatial density. This is achieved by fitting a two-dimensional Gaussian kernel density estimator (KDE) to the cluster's spatial layout. What sets ASteCA apart from similar methods is its ability to operate without preset initial values, though they can be provided for semi-automatic operation. The tool ensures consistent convergence. This approach is less dependent on the binning of the area because it determines the KDE's bandwidth using Scotts rule Scott (1992), a recognized standard. It also simultaneously calculates the maximum density estimate in both spatial dimensions, reducing the impact that densely packed areas might have on pinpointing the central coordinates. Moreover, the process is adaptable to various coordinate systems and is equally effective with data expressed in pixels or degrees.

Figure 1 represents the re-estimated center using the ASteCA method (as well as the images of the clusters taken from the STScI Digitized Sky Survey[4]). According to our analysis, the new centers of NGC 7031 are less by about $0^{\circ}.1564$ in right ascension and exceeded by about $0^{\circ}.0013$ in declination, and in the same manner for NGC 7086 our obtained right ascension is less by about $0^{\circ}.0153$ in right ascension and exceed with $0^{\circ}.083$ in declination as compared with those obtained with Dias et al. (2002) and WEBDA. Table 2 reports the updated

---

[4]https://archive.stsci.edu/cgi-bin/dss_form

centers of the clusters in the equatorial $(\alpha,\ \delta)$ and Galactic $(l,\ b)$ coordinate systems. Figure 2 displays in three photometric bands G, G_{BP}, and G_{RP} the uncertainty in photometric magnitudes 0.05 for $G \leq 21$ mag.
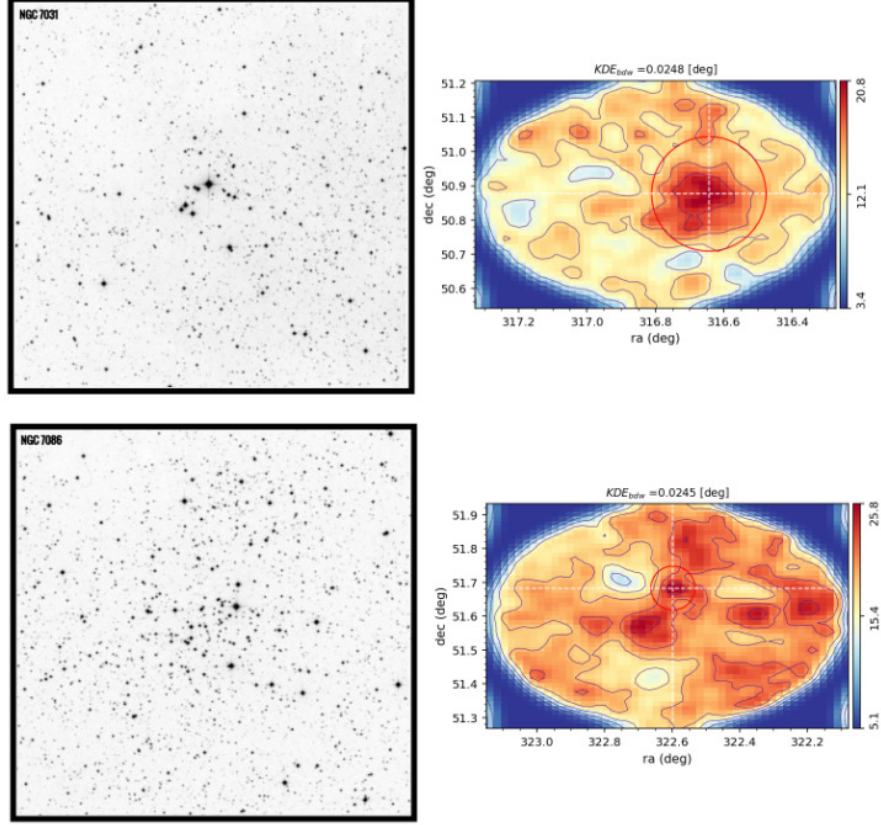

Figure 1. The images (left panel) and the contour maps (right panel) show the centers according to the Kernel density estimation technique (KDE) applied by ASteCa of both NGC 7031 (top) and NGC 7086 (bottom).

3.2. Radial stellar surface density and cluster radii

To investigate the inner structural parameters of NGC 7031 and NGC 7086, we analyze the radial density profiles (RDP). The RDP is often calculated by dividing the number of stars that lie inside each ring by its area, and then creating concentric circular rings around the designated cluster center with increasing radius values, i.e., the observable regions of each cluster were divided into many
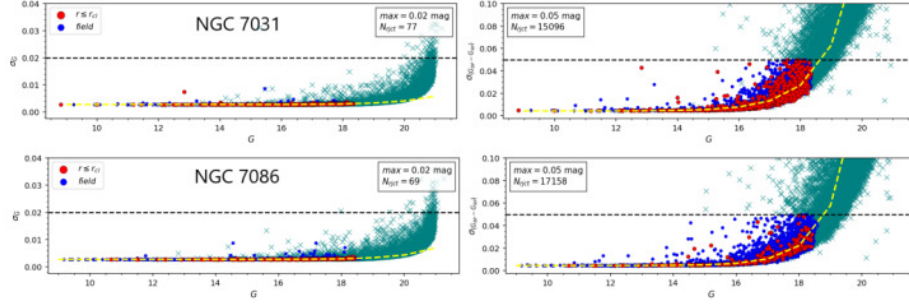
Figure 2. Photometric uncertainties in Gaia bands (G, G_{BP}, and G_{RP}) with G magnitudes which are used to clean the cluster field stars by rejection stars (the green x symbol) with uncertainties more than 0.02 in G mag and 0.05 in color-magnitude G_{BP}-G_{RP}, respectively.

Table 2. Our new center estimate of NGC 7031 and NGC 7086.

Coordinates	NGC 7031	NGC 7086
α	$21^{\rm h}\ 06^{\rm m}\ 34^{\rm s}.46$	$21^{\rm h}\ 30^{\rm m}\ 23^{\rm s}.33$
δ	$50^{\rm d}\ 52^{\rm m}\ 35^{\rm s}.08$	$51^{\rm h}\ 40^{\rm m}\ 59^{\rm s}.20$
l^{o}	$91^{\circ}.5932$	$94^{\circ}.8009$
b^{o}	$2^{\circ}.3251$	$0^{\circ}.2690$

concentric rings that centered around the cluster center. The number density (r_i) in the ith zone may be found using the formula $(r_i = N_i A_i)$, where (N_i) is the number of stars and (A_i) is the ith zone's area. First, we adopted the new central coordinates of the clusters as given in Table 2 and downloaded new row data with 14.00 and 12.00 arcmin for both clusters respectively with Gaia DR3 and then, following Perren et al. (2015), generated concentric square rings using an underlying 2D histogram or grid in the observed frame's positional space. This positional histogram's bin width is equal to 1% of the spatial dimension that covers the smallest range in the observed frame. Therefore, for each cluster, the fitted RDP could be utilized with King's profile (King, 1962) equation,

$$\rho(r) \;=\; f_{bg} + \frac{f_o}{1 + (r/r_{\rm c})^2}, \tag{1}$$

where f_o is the central surface density (i.e., maximum density), f_{bg} is the background surface density, and r_c is the core radius (distance from the obtained center to the point at which the value of $\rho(r)$ becomes half of the central density f_o). As seen in Figure 3, we created two RDPs using King's model for both clusters, which was fitted using Equation (1). Table 3 lists our obtained results with RDPs of NGC 7031 and NGC 7086.

Comparing our results of f_o and f_{bg} with those of Yontan et al. (2019), we found a large difference between our and their results in central and background densities in both clusters. We claim that their results are not reliable because the values of f_o are less than f_{bg}, which is not consistent with the King model; rather than their results depend on Gaia DR2, which clear from Figure 3 of Yontan et al. (2019). So, we are satisfied with our results from RDP (Figure 3) using the recent data of Gaia DR3, which is consistent with the King model (i.e., $f_o > f_{bg}$). Therefore, their error in estimating the King model fitting parameters (i.e., f_o, f_{bg}, and r_c) on both clusters may reflect on core, limiting, and tidal radii.

The limiting radius (r_{cl}; arcmin) in expansion may be defined as the point into which the gravitational pull from the Galaxy center as well as the gravitational acceleration from the cluster center (von Hoerner, 1957). r_{cl} was calculated by comparing $\rho(r)$ to a background density level ρ_b (i.e., $\rho_b = f_{bg} + 3\sigma_{bg}$), where the uncertainty of f_{bg} is σ_{bg}. The following formula provides the value of r_{cl} (Bukowiecki et al., 2011).

$$r_{cl} = r_c \sqrt{\frac{f_o}{3\,\sigma_{bg}} - 1}. \tag{2}$$

According to Table 3, we found a difference in numerical values of the core radius (r_c) for both clusters as compared with those obtained by Hunt & Reffert (2024), which may account for the difference in the distance and the number of members.

3.3. Tidal radii

According to von Hoerner (1957), the tidal radius is the distance from the cluster center at which the gravitational acceleration created by the cluster equals the tidal acceleration caused by the parent galaxy. Jeffries et al. (2001) have introduced a relation between the tidal radius (r_t; pc) and the total mass (M_C; M$_\odot$) as (see section 5)

$$r_t = 1.46 \sqrt[3]{M_C}. \tag{3}$$

Our estimated values of tidal radii (pc) for both clusters NGC 7031 and NGC 7086 are 14.94 ± 0.26 and 12.30 ± 0.29, respectively.

Empirically, the limiting radius lags between $2 - 7$ times the core radius. Therefore, we obtained values of 10.04 and 3.91 arcmin for NGC 7031 and NGC 7086, respectively. On the other hand, other inner structural parameters may be deduced for OCs. First, the concentration parameter ($C = r_{cl}r_c$) King (1966) defined the C as the ratio of the cluster limiting and core radii and can be indicated by the concentration of the cluster's center. Santos-Silva & Gregorio-Hetem (2012) reversed King's definition of the C parameter from King (1966) and expect that young clusters will have low C values since many of their
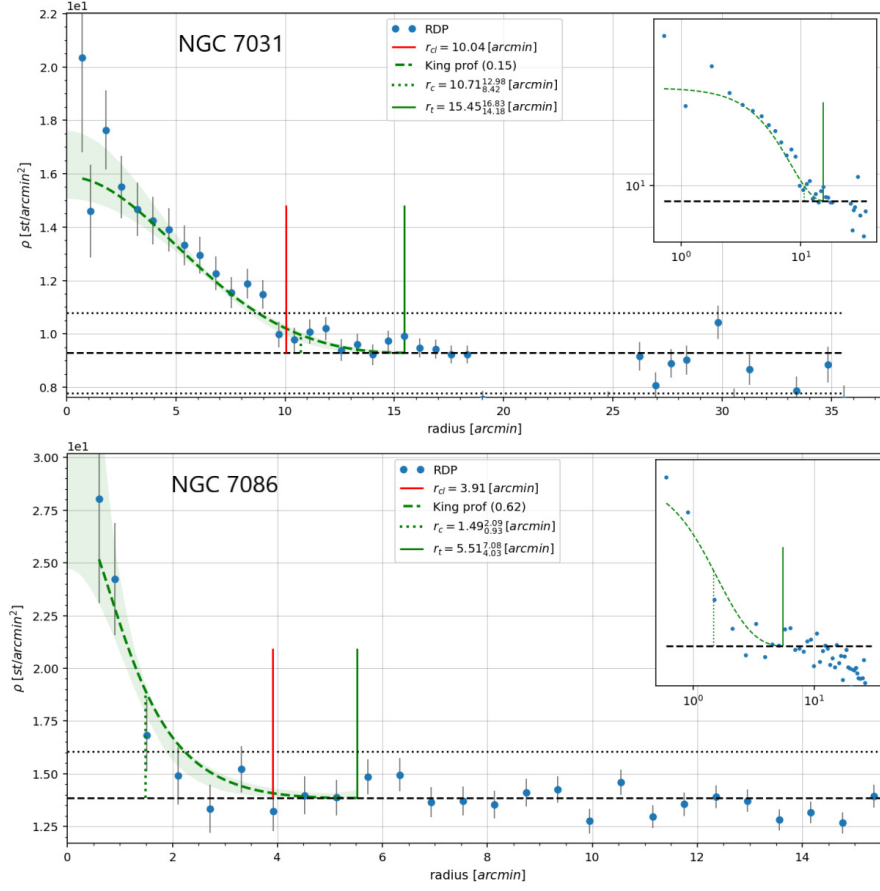
Figure 3. The RDPs of both NGC 7031 (top) and NGC 7086 (bottom). The dashed green lines were applied with the King's density distribution model, the horizontal dashed lines denote the background field density (f_{bg}; stars arcmin^{-1}). The vertical dotted green lines, vertical solid red lines, and vertical solid green lines indicate the cluster core (r_c), limiting (r_{cl}), and tidal (r_t) radii (in arcmin), respectively.

members are still concentrated in the center and haven't had enough time to spread out of their borders. Based on Table 3, we arrived at a reasonable C range (Santos-Silva & Gregorio-Hetem, 2012) as 1.20 ± 0.08 and 4.20 ± 0.49. Second, Bonatto & Bica (2009) defined density parameters for compact OCs known as the density contrast parameter (i.e., $\delta_c = 1 + f_o f_{bg}$) and give values $7 \leq \delta_c \leq 23$. Our computed δ_c are 2.760 ± 0.60 and 2.986 ± 0.58 for both clusters respectively, and we may conclude that NGC 7031 and NGC 7086 are scattered concerning their background density.

Table 3. Our inner structural properties of NGC 7031 and NGC 7086 as compared with (1) Yontan et al. (2019) and (2) Hunt & Reffert (2024).

Parameters	NGC 7031	NGC 7086	References
(f_o; stars arcmin^{-2})	16.319 ± 0.780	24.366 ± 5.473	Current work
	1.978 ± 0.059	3.602 ± 0.280	(1)
(f_{bg}; stars arcmin^{-2})	9.276 ± 0.402	12.381 ± 0.228	Current work
	4.006 ± 0.443	5.009 ± 0.171	(1)
(r_c; arcmin)	$10.71_{8.42}^{12.98}$	$1.49_{0.93}^{2.09}$	Current work
	3.241 ± 1.816	1.517 ± 0.255	(1)
(r_c; pc)	2.19 ± 0.68	0.41 ± 0.02	Current work
	2.23	2.51	(2)
(r_{cl}; arcmin)	10.04	3.91	Current work
(r_{cl}; pc)	2.05 ± 0.70	1.08 ± 0.03	Current work
	9.97	10.66	(2)
(r_t; arcmin)	$15.45_{14.18}^{16.83}$	$5.51_{4.03}^{7.08}$	Current work
(r_t; pc)	3.16 ± 0.56	1.51 ± 0.18	Current work
	9.974	10.656	(2)
C	1.20 ± 0.08	4.20 ± 0.49	Current work
δ_c	2.760 ± 0.60	2.986 ± 0.58	Current work

4. CMDs and member stars of the clusters

The highly accurate determination of cluster star members can be achieved by combining radial velocities, distances, and proper motions, either alone or in combination. Large spectroscopic surveys created for various objectives can now be used to identify cluster members (Allende Prieto et al. (2008); Gilmore et al. (2012); De Silva et al. (2015)). Spectroscopic observations require a telescope-time-focused methodology, which limits our ability to comprehend the characteristics of several clusters. Furthermore, no spectroscopic survey to determine the radial velocities of all Milky Way stars is scheduled. Fortunately, many techniques exist to distinguish cluster members from field stars because cluster stars share the same spatial origin (e.g. Krone-Martins & Moitinho (2014); Javakhishvili et al. (2006); Balaguer-Núñez et al. (1998)). These techniques typically consider the proper motions of the stars.

Perren et al. (2015) with the ASteCA code used two methods to estimate the overall number of likely cluster members. The first uses the integral of the RDP from zero to rt above the estimated star field density and is based on the three-parameter (3P) King profile fitting. Only a decent tidal radius and convergence of the 3P fit are required for this method to be effective; otherwise, the result may be greatly overestimated. The second method is based on a straightforward star count (n_{fl}), or the approximate number of field stars inside the cluster region, is obtained by multiplying the field density value (d_{field}) by the area (A_{cl}) of the cluster (which is determined by the r_{cl} radius). After deducting this

amount from the actual number of stars inside the r_{cl} boundary (n_{cl+fl}), the final estimated number of cluster members, n_{cl}, is obtained:

$$n_{cl} = n_{cl+fl} - d_{field} \, A_{cl}. \tag{4}$$

Both approaches depend on the degree of completeness since they provide the approximate number of members down to the lowest observed magnitude.

By looking for a significant stellar over-density and contrasting it with the surrounding stellar field, the membership probability is assigned using the proper motion and parallax that are accessible from the Gaia DR3 database with the ASteCA code. In this investigation, the cluster most probable candidates are limited to stars with membership probabilities $P \geq 50\%$. As a result, we have 613 and 226 candidates for NGC 7031 and NGC 7086, respectively.

We employed the ASteCA code and the PARSEC v1.25 of Bressan et al. (2012) theoretical isochrones for each CMD of the clusters, as well as the Gaia DR3 photometric magnitudes (G, G_{BP}, G_{RP}) for our candidates, to derive the cluster metallicity (Z) and ages (in a log scale). Therefore, the best-suited metallicities are 0.01189 ± 0.00023 & 0.01121 ± 0.00025 and the ages (log yr^{-1}) are 8.468 ± 0.007 & 8.617 ± 0.021 for NGC 7031 and NGC 7086, respectively. Our fitted CMDs for $(G_{BP} - G_{RP}, G)$ mag are shown in Figure 4.

We approximated the reddening with magnitudes G_{BP} and G_{RP} from CMDs using most likely members from Gaia DR3 using the formula $E(G_{BP} - G_{RP}) = 1.289 \times E(B - V)$ (Cardelli et al., 1989). After correcting the observed data for reddening $A_G = 2.74 \times E(B-V)$ using a line-of-sight extinction coefficient (A_G) in the G-band calculated by Casagrande & VandenBerg (2018) and Zhong et al. (2019), we were able to obtain A_G values of 2.55 & 1.93 and $E(G_{BP} - G_{RP})$ of 1.197 ± 0.08 & 0.908 ± 0.05 for NGC 7031 and NGC 7086, respectively.

The distance moduli $(m - M)$ for NGC 7031 and NGC 7086 are 9.229 ± 0.037 and 9.869 ± 0.001 mag, respectively. This indicates that the photometric distances $(d_{phot}; \text{pc})$ in the same manner are approximately 701 ± 26 and 942 ± 31, which are slightly different from those obtained by Yontan et al. (2019).

We calculated the mean proper motion on both sides $(\mu_\alpha^\star, \mu_\delta)$ in the following with adopted members using the stellar space distribution as illustrated in the upper and lower panels of Figure 5, and the results yielded the following numerical values $(-3.03, -2.53;$ NGC 7031$)$ and $(-3.09, -3.26;$ NGC 7086$)$ in mas yr^{-1} units. On the other hand, their Gaussian distributions are displayed in the left and right panels of Figure 6 with numerical values $(0.571;$ NGC 7031$)$ and $(0.622;$ NGC 7086$)$ in millarcsec units. Then the reflected astrometric distances $(d_{plx}; \text{pc})$ are 1752 ± 42 and 1608 ± 40, which are consistent with those obtained by Hunt & Reffert (2024), Yontan et al. (2019), and Cantat-Gaudin et al. (2018). All our astrophysical parameters devoted to both clusters are represented in Table 4 as compared by different authors.

We deduce that the distances to the Galactic center R_{gc} should be included based on our estimated d_{phot} distances, which are defined as
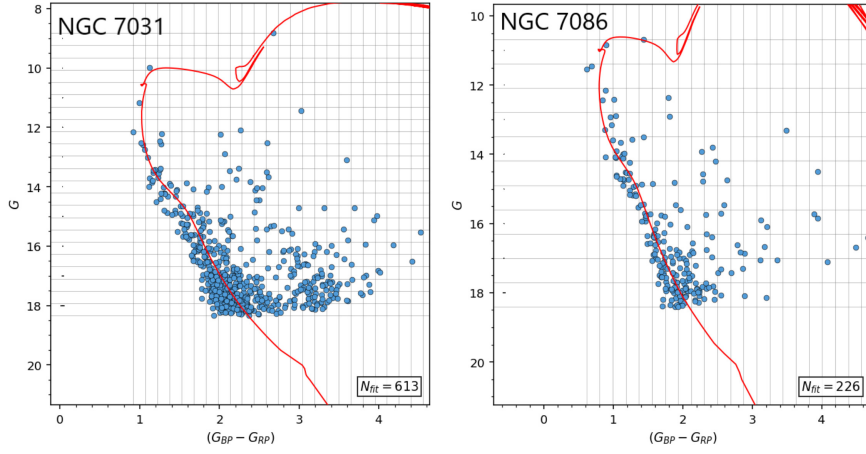
Figure 4. The CMDs of NGC 7031 (left) and NGC 7086 (right). The fitted extinction was corrected by Bressan et al. (2012).

$$R_{gc} = \sqrt{R_o^2 + (d\ cosb)^2 - 2\ R_o\ d\ cosb\ cosl} \tag{5}$$

where $R_o = 8.20 \pm 0.10$ kpc (Bland-Hawthorn et al., 2019). The following relationships can be used to calculate the projected distances toward the Galactic plane $(X_\odot, Y_\odot)$ and the distance away from the Galactic plane $(Z_\odot)$. The findings are shown in Table 4.

$$X_\odot = d\cos b\cos l, \quad Y_\odot = d\cos b\sin l, \quad Z_\odot = d\sin b. \tag{6}$$

5. Luminosity and mass functions

Each cluster's members are formed under similar physical conditions (same morphology) from the same molecular cloud at the same time. Therefore, the OC luminosity function (LF), which may be viewed as a projection of its CMD on the magnitude axis, indicates the distribution of member stars according to different absolute magnitude intervals.

Based on our previously mentioned NGC 7031 and NGC 7086 worksheet row data from DR3 Gaia Collaboration (2022) we have updated central positions, and astrophysical and photometric parameters, on this context, we have computed LF of both clusters as seen in the upper panel of Figure 7, where the
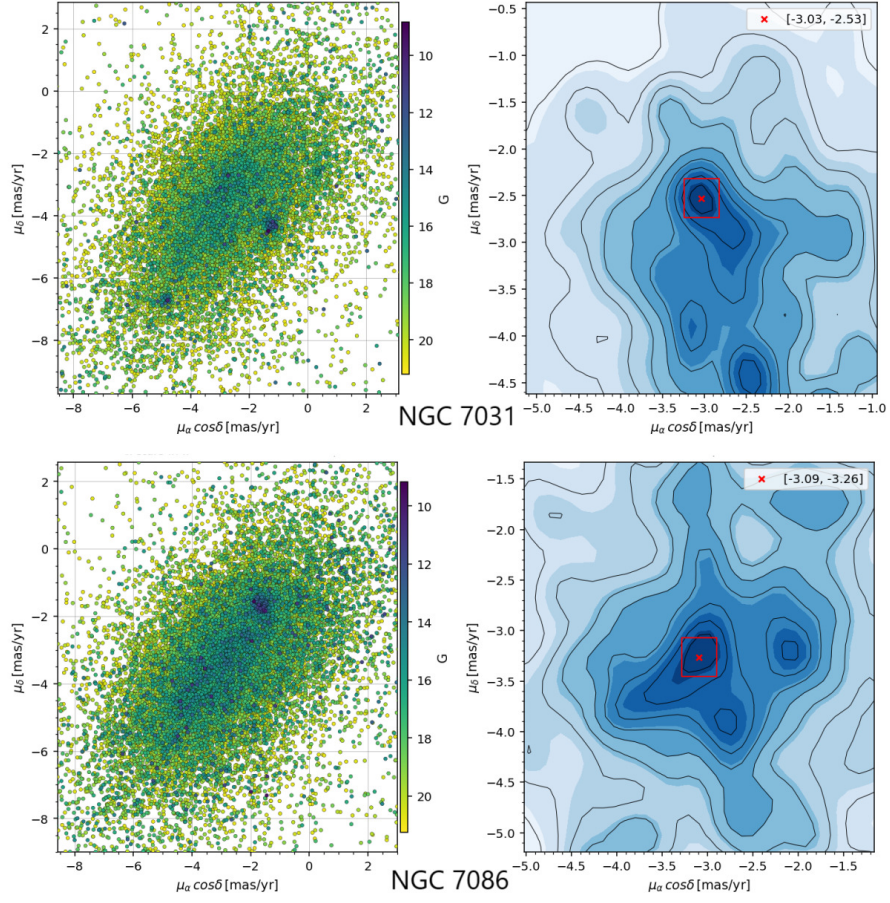
Figure 5. Mean proper motion distribution and their contours for NGC 7031 (top) and NGC 7086 (bottom).

estimated average values of absolute magnitudes ($\overline{M_G}$; mag) of each cluster are 7.51 ± 0.36 & 6.54 ± 0.39 for NGC 7031 & NGC 7086, respectively.

Empirically, the well-established mass-luminosity relation (MLR) links LF and mass function (MF) together. Additionally, absolute magnitudes (M_G; mag) and collective masses (M_C; $M\odot$) attributed to adopted isochrones on CMDs for estimated ages, distance modulus, and reddening are taken into account. These findings were reported by Evans et al. (2018).

The initial mass function (IMF), which is defined as an initial arrangement of the star's masses, can be studied with great benefit from OCs mass spectrum, which contains both very low and very high mass stars (Scalo (1998); Phelps &
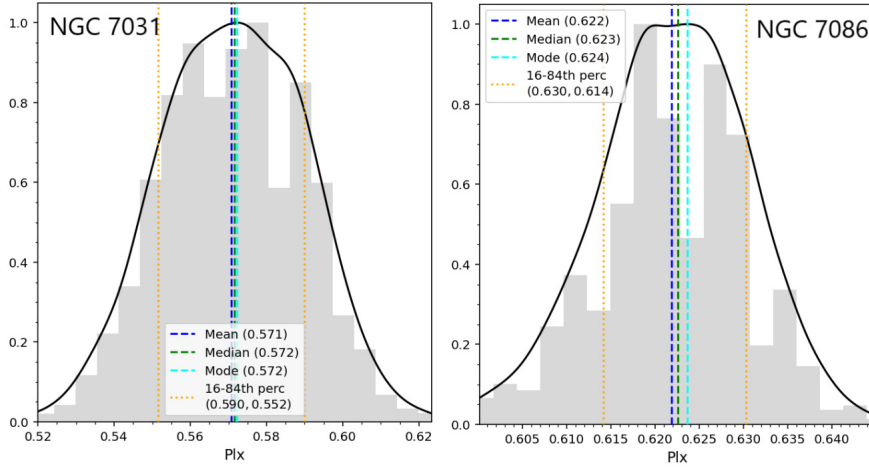
Figure 6. Parallax Gaussian distribution fitting diagrams for NGC 7031 (left) and NGC 7086 (right).

Janes (1993); Durgapal & Pandey (2001); Piatti et al. (2002); Piskunov et al. (2004); Sung & Bessell (2004); Yadav & Sagar (2002); Yadav & Sagar (2004); Bisht et al. (2017); Bisht et al. (2019)). The IMF, or present-day mass function theoretically, was defined by Salpeter (1955) as the total number (dN) the density of stars spread along a logarithmic mass scale in a mass bin (dM) with the central mass (M),

$$Log\left(\frac{dN}{dM}\right) = -\alpha\ Log(M) + \text{constant}, \tag{7}$$

where α is a dimensionless quantity that describes the slope of the straight line representing the MF-like lower panel of Figure 7, and it is dedicated as a characteristic of dynamical evolution for massive stars ($> 1M_\odot$). Salpeter's power law states that as mass increases, there are fewer stars in each mass range. Our calculated slopes from least-square fitting the MF data are 2.73 ± 0.25 & 2.67 ± 0.32 for NGC 7031 and NGC 7086, respectively, and agree with Salpeter (1955) results.

Our study indicates that the stars with the following (M_G; mag) ranges are included in the MFs calculations: ($-0.405 \geq (M_G) \geq 9.116$ & $1.333 \geq (M_C) \geq 6.057$; NGC 7031) and ($0.806 \geq (M_G) \geq 8.545$ & $1.915 \geq (M_C) \geq 5.038$; NGC 7086). The average mass ($\overline{M_C}$), total mass (M_C), and slopes (α) are provided in Table 5.

Table 4. Our obtained astrophysical and photometric parameters of NGC 7031 and NGC 7086 as compared with those of (1) Hunt & Reffert (2024), (2) Yontan et al. (2019) and (3) Cantat-Gaudin et al. (2018).

Parameters	NGC 7031	NGC 7086	References
N	613	226	Current work
	264	963	(1)
	208	543	(2)
	171	622	(3)
$(\overrightarrow{\mu_\alpha^\star};$ mas yr$^{-1})$	-3.03	-3.09	Current work
	-1.242 ± 0.122	-1.656 ± 0.148	(3)
$(\overline{\mu_\delta};$ mas yr$^{-1})$	-2.53	-3.26	Current work
	-4.205 ± 0.130	-1.629 ± 0.143	(3)
$(d_{plx};\ pc)$	1752 ± 42	1608 ± 40	Current work
	1402	1667	(1)
	1365^{+164}_{-216}	1616^{+225}_{-312}	(3)
$(d_{phot};\ pc)$	701 ± 26	942 ± 31	Current work
Z	0.01189 ± 0.00023	0.01121 ± 0.00025	Current work
$log(age\ yr^{-1})$	8.468 ± 0.007	8.617 ± 0.021	Current work
A_G	2.55	1.93	Current work
$E(B-V)_{mag}$	0.929 ± 0.006	0.704 ± 0.001	Current work
$E(G_{BP} - G_{RP})_{mag}$	1.197 ± 0.08	0.908 ± 0.05	Current work
	1.254	1.277	(1)
$(m-M)_{mag}$	9.229 ± 0.006	9.869 ± 0.001	Current work
$(X_\odot;$ kpc)	-0.050 ± 0.007	-0.135 ± 0.012	Current work
	-0.033	-0.128	(1)
$(Y_\odot;$ kpc)	1.750 ± 0.042	1.602 ± 0.040	Current work
	1.401	1.662	(1)
$(Z_\odot;$ kpc)	0.071 ± 0.008	-0.008 ± 0.009	Current work
	0.056	0.006	(1)
$(R_{gc};$ kpc)	8.432 ± 0.092	8.487 ± 0.093	Current work

6. Evolving times and escape velocity

The interactions between stars in OCs result in energy exchange (Inagaki & Saslaw (1985); Baumgardt & Makino (2003)). The spatial distribution of OCs is less dense than that of globular clusters. In the event of a force of contraction and/or destruction, massive stars exhibit mass segregation towards the cluster core, compared to fainter stars. Numerous OCs have recently been observed to exhibit this phenomenon (Piatti (2016); Zeidler et al. (2017); Dib & Basu (2018); Rangwal et al. (2019); Bisht et al. (2020); Joshi et al. (2020)). Following a Maxwellian stability equilibrium (i.e., dynamical evolution), the cluster's kinetic energy (velocity distribution) approaches one (Yadav et al. (2013); Bisht et al. (2019)) within dynamical relaxation time (T_{relax}; Myr) which is the characteristic time required for dynamical evolution to be completed. T_{relax} depends
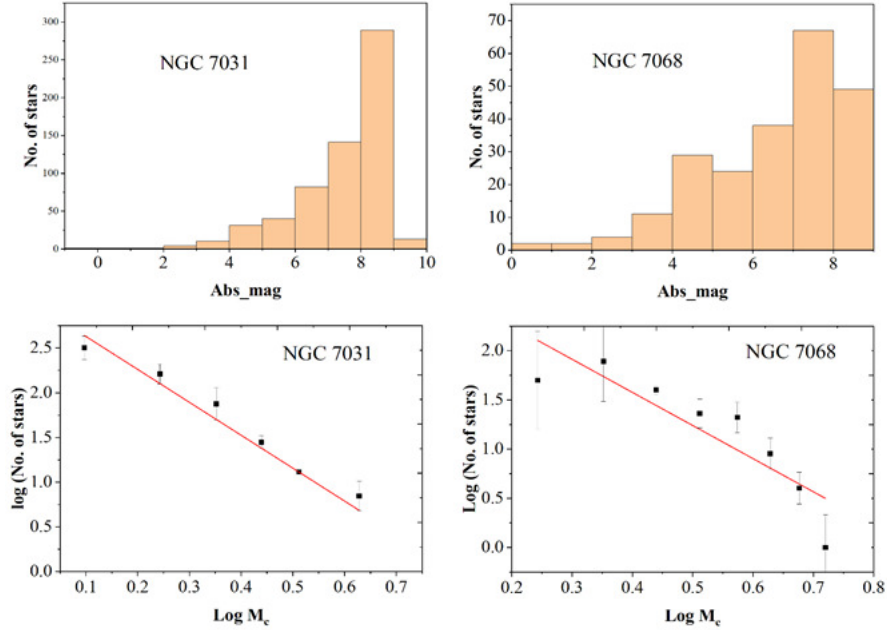
Figure 7. The true LFs for NGC 7031 and NGC 7086 are shown in the top panel. These LFs were constructed by taking the cluster's $(m - M)$ into consideration while converting the observed G magnitudes of its member stars into absolute magnitudes M_G. The lower panel displays MFs that were obtained using the most likely members; Salpeter's power-law fitting is indicated by solid lines in this panel.

on both cluster diameter and the number N of member stars (Lada & Lada, 2003), and according to Spitzer & Hart (1971) is given by

$$T_{relax} = \frac{8.9 \times 10^5 \ N^{1/2} \ R_h^{3/2}}{\sqrt{\overline{M}_C} \ log(0.4 \ N)}, \tag{8}$$

where R_h, which can be determined using the transformation outlined by Šablevičiūtė et al. (2006), is the radius (in pc) containing about 50% of the cluster mass,

$$R_h = 0.547 \times r_c \times \left(\frac{r_t}{r_c}\right)^{0.486}, \tag{9}$$

where the tidal and core radii are denoted, respectively, by r_c and r_t. Therefore, the derived (R_h; pc) values are 3.07 ± 0.57 and 0.97 ± 0.01. In the same manner the (T_{relax}; Myr) are 1.515 and 0.267 for both NGC 7031 and NGC 7086, respectively. In addition to the relaxation time, we focus on estimating the evaporation time ($\tau_{ev} \approx 10^2 T_{relax}$; Myr), which is how long it takes to

Table 5. Our estimated average absolute magnitudes, average mass, total mass, and the IMF slopes for NGC 7031 and NGC 7086 as expressed with recent literature (1) Hunt & Reffert (2024).

Parameters	NGC 7031	NGC 7086	References
$(\overline{M_G}; mag)$	7.51 ± 0.36	6.54 ± 0.39	Current work
$(M_C; M_\odot)$	1072 ± 33	598 ± 25	Current work
	1403 ± 124	4271 ± 300	(1)
$(\overline{M_G}; M_\odot)$	1.75	2.64	Current work
α	2.73 ± 0.25	2.67 ± 0.32	Current work

Table 6. Table 6: Our dynamical evolution times and escape velocity for NGC 7031 and NGC 7086.

Parameters	NGC 7031	NGC 7086
T_{relax} (Myr)	1.515	0.276
τ_{ev} (Myr)	151.50	27.60
τ	194	1550
V_{esc} (km s^{-1})	251 ± 16	447 ± 21

evacuate every member star from internal stellar encounters (Adams & Myers, 2001). By calculating the dynamical evolution parameter (i.e., $\tau = age/T_{relax}$), we may characterize and specify the dynamic state of clusters. We concluded that our $\tau \gg 1$ for every cluster, therefore, these clusters are considered to be dynamically relaxed OCs.

Low-mass stars continue to set off the cluster, primarily at slow speeds via Lagrange points Küpper et al. (2008). The escape velocity (V_{esc}; km s^{-1}) of rapid gas removal from the cluster when it remains bound in the face is $\left(V_{esc} = R_{gc}\sqrt{2\ G\ M_C\ /\ 3r_t^3}\right)$ (Fich & Tremaine (1991); Fukushige & Heggie (2000)), where the gravitational constant is $G = 4.3 \times 10^{-6}$ kpc $M_\odot^{-1}$ (km s^{-1})^2. In light of these achieved dynamical parameters, different times, and escaping velocities are shown in Table 6.

7. Ellipsoidal motion and the kinematical structure

To evaluate the coherent and uniform movements within a confined spatial region of gravitationally bound stellar assemblies in the Galactic framework, we applied a computational methodology formulated by Elsanhoury et al. (2018) and Bisht et al. (2020). This approach was utilized to determine the velocity ellipsoid parameters (VEPs) and the overall kinematics of the clusters. The

analysis focused on cluster members identified by their celestial coordinates (α_i, δ_i) with their proper motion ($\mu_{\alpha_i}^{\star}$, μ_{δ_i}), distance (d_i), and radial velocity (V_r) with specific velocities (Hunt & Reffert, 2024) being 12.05 ± 7.69 km s^{-1} (NGC 7031) and -16.10 ± 3.16 km s^{-1} (NGC 7086). Furthermore, we investigated their spatial velocity components (V_x, V_y, V_z; km s^{-1}) along the x, y, and z axes of a solar-centric coordinate system.

The determination of space velocity components in Galactic coordinates (U, V, W; km s^{-1}) employs the transformation equations outlined by Liu et al. (2011) and their distribution is shown in Figure 8.

$$U = -0.0518807421V_x - 0.8722226427V_y - 0.4863497200V_z, \tag{10}$$

$$V = +0.4846922369V_x - 0.4477920852V_y + 0.7513692061V_z, \tag{11}$$

$$W = -0.8731447899V_x - 0.1967483417V_y + 0.4459913295V_z. \tag{12}$$
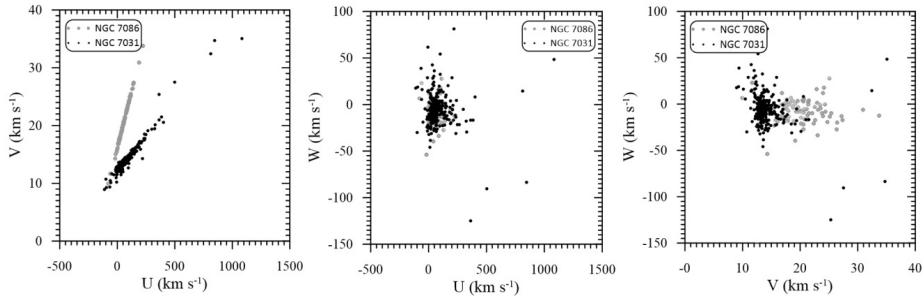

Figure 8. The distribution of the spatial velocity components for the member stars of NGC 7031 (black dots) and NGC 7086 (gray dots) in the Galactic coordinates.

Additionally, the apex coordinates of the cluster are ascertained through the apex diagram (AD) method, as illustrated in Figure 9, employing formulae for constructing the AD diagram as described by Chupina et al. (2001) and Chupina et al. (2006):

$$A_o = \tan^{-1}\left(\frac{\bar{V}_y}{\bar{V}_x}\right), \tag{13}$$

and

$$D_o = \tan^{-1}\left(\frac{\bar{V}_z}{\sqrt{\bar{V}_x^2 + \bar{V}_y^2}}\right). \tag{14}$$
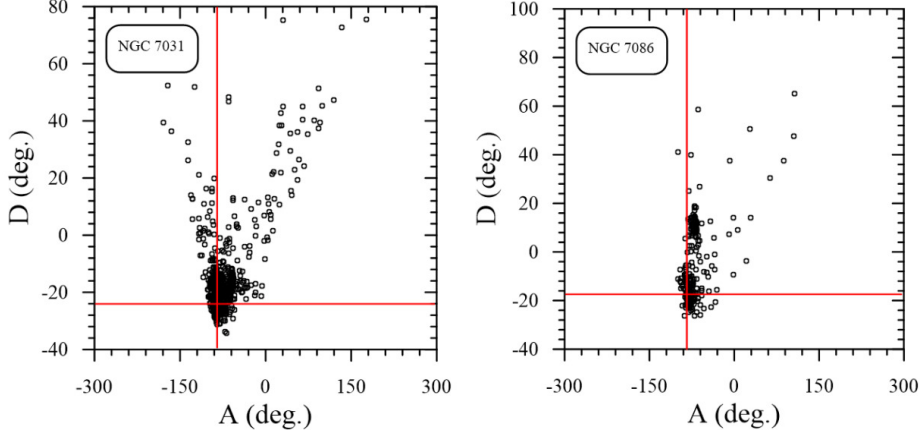
Figure 9. The AD diagram for NGC 7031 (left panel) and NGC 7086 (right panel) with a cross mark denoting the location of their convergent point (A_o, D_o).

The AD diagram facilitates an analysis of the cluster's kinematic structure and the identification of its internal kinematic substructures. This diagram, created from the individual apexes of stars, showcases the distribution of stars within the equatorial coordinate system, where the apex equatorial coordinates (in degrees) are labeled A_o (right ascension) and D_o (declination). These coordinates result from solving a geometrical problem involving the intersection points of stars' spatial velocity vectors with the celestial sphere.

Concerning other kinematic parameters, the cluster center $(x_c, y_c, z_c;$ kpc) is derived by calculating the mass center of N stars using equatorial coordinates (α_i, δ_i) and distance d_i. The solar motion elements, indicating the Sun's velocity relative to the star group being studied, are defined as

$$U_\odot = -\bar{U}, \quad V_\odot = -\bar{V}, \quad \text{and} \quad W_\odot = -\bar{W}$$

.

Additionally, this study pioneers in estimating the solar apex location (l_A, b_A) in Galactic coordinates and their corresponding equatorial coordinates (α_A, δ_A) for both NGC 7031 and NGC 7086 OCs. We obtained the numerical kinematical results and the solar motion elements arranged in Table 7. The angular separation angle between NGC 7031 and NGC 7086 is about $3^o.81$ (i.e., 55.08 ± 7.42 pc) as depicted in Figure 10.

8. Conclusion

In the current study, we used Gaia DR3 to determine the photometric and astrometric properties of the star clusters NGC 7031 and NGC 7086. With
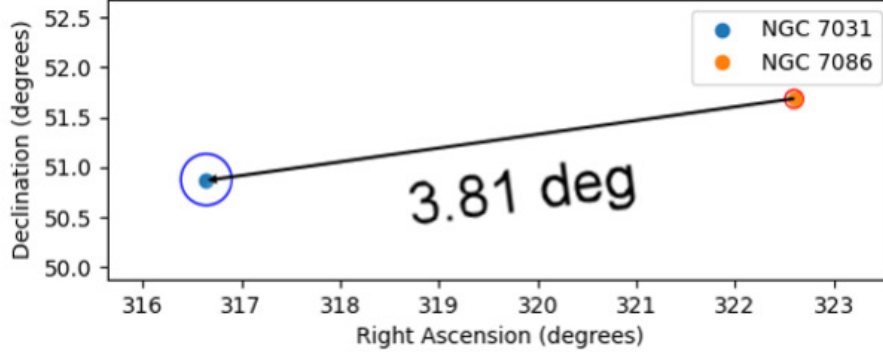
Figure 10. The angular separation between NGC 7031 and NGC 7086.

Table 7. Our obtained results of VEPs for NGC 7031 and NGC 7086 with their solar motion elements.

Parameters	NGC 7031	NGC 7086
$\overline{V}_x$ (km s^{-1})	9.51 ± 0.32	12.78 ± 0.28
$\overline{V}_y$ (km s^{-1})	-90.27 ± 9.50	-77.96 ± 8.83
$\overline{V}_z$ (km s^{-1})	-40.46 ± 6.36	-24.93 ± 4.99
A_o	$-83^{\circ}.99 \pm 0^{\circ}.11$	$-80^{\circ}.69 \pm 0^{\circ}.11$
D_o	$-24^{\circ}.02 \pm 0^{\circ}.20$	$-17^{\circ}.51 \pm 0^{\circ}.24$
$\overline{U}$ (km s^{-1})	97.91 ± 9.90	79.46 ± 8.91
$\overline{V}$ (km s^{-1})	14.63 ± 3.83	22.37 ± 4.73
$\overline{W}$ (km s^{-1})	-8.58 ± 0.34	-6.94 ± 0.38
x_c (kpc)	2.276 ± 0.048	1.860 ± 0.043
y_c (kpc)	-2.148 ± 0.046	-1.423 ± 0.038
z_c (kpc)	3.850 ± 0.062	2.963 ± 0.054
$S_{\odot}$ (km s^{-1})	99.37 ± 9.97	82.84 ± 9.10
$(l_A, b_A)^{\circ}$	-8.50, 4.95	-15.73, 4.80
$(\alpha_A, \delta_A)^{\circ}$	-83.99, 24.02	-80.70, 17.52

membership probabilities $P \geq 50\%$, we assessed the most probable member stars to be 613 and 226 for respective clusters. We derived all the parameters using these Gaia-based likely members. Our results are in good agreement with the estimated parameters found in several of the most recent prior investigations. Under or overestimated numerical values in Tables 3 and 4 depending on the number of possible candidates, method of estimation and the data used. The following summarizes the main findings of the current studies:

• The distances from the cluster centers where the density of the cluster merged with the background density are named the clusters' limiting radius r_{cl}.

Our estimates are 10.04 and 3.91 arcminutes for NGC 7031 and NGC 7086, respectively.

• We created the proper motion and parallax histograms of these Gaia-based probable members by utilizing the most likely members of the two clusters that were found using the Gaia DR3 mean proper motion data. The results we computed are as follows:

⋆ $(\overline{\mu_\alpha^\star}, \overline{\mu_\delta})_{\text{NGC7031}}$ is about (-3.03, -2.53; mas yr^{-1}), Plx$_{\text{NGC 7031}}$ is equal to 0.571 mas, and the corresponding distance d$_{\text{plx}}$ (NGC 7031) = 1752 ± 42 pc.

⋆ $(\overline{\mu_\alpha^\star}, \overline{\mu_\delta})_{\text{NGC7086}}$ is about (-3.09, -3.26; mas yr^{-1}), Plx$_{\text{NGC 7086}}$ is equal to 0.622 mas, and the corresponding distance d$_{\text{plx}}$ (NGC 7086) = 1608 ± 40 pc.

• The ages (in a log scale) of NGC 7031 and NGC 7086 were determined to be 8.468 ± 0.007 and 8.617 ± 0.021, by fitting their CMDs with the theoretical isochrones of Bressan et al. (2012) using Gaia DR3. According to Gaia photometry, their isochrone-based distances are 701 ± 26 and 942 ± 31 pc for respective clusters. The distances of both clusters from the galactic plane, $Z_\odot$, as well as their projected distances from the Sun, $X_\odot$, and $Y_\odot$, and the galactic centers R_{gc}, were then calculated and are all shown in Table 4.

• Total masses (in solar units) are 1072 ± 33 and 598 ± 25 for respective clusters. As compared with Hunt & Reffert (2024) for total mass (M_C; $M\odot$) for both clusters, we found a slight difference in NGC 7031 due to our estimation and Hunt & Reffert (2024), on the other hand, a large difference in NGC 7086 which we recall for the number of candidates (i.e., 226; current work & 963; Hunt & Reffert (2024)). The initial mass function (IMF) slope was determined, i.e. $\alpha_{NGC7031} = 2.73 \pm 0.25$ and $\alpha_{NGC7086} = 2.67 \pm 0.32$, and they were found to be reasonably consistent with the value reported by Salpeter in 1955.

• We deduced that NGC 7031 and NGC 7086 are dynamically relaxed clusters with notable mass segregation based on the computation of their relaxation time.

• We presented the first complete estimation of the space velocities and kinematic parameters of both clusters, therefore, the convergent points (-83º.99 ± 0º.11, -24º.02 ± 0º.20) and (-80º.69 ± 0º.11, -17º.51 ± 0º.24) with respective clusters.

• Ultimately, we estimate that the age difference between NGC 7031 and NGC 7086 is 120 Myr, the linear separation between the two clusters is about 55.08 ± 7.42 pc and the distance difference along the line of sight is 228 pc. Since these findings do not meet the requirements for a binary cluster, we conclude that the two clusters are not genuine binary clusters and are most likely not produced from the same Giant Molecular Cloud (GMC).

Data availability: We have used the different data sets for the analysis of NGC 7031 and NGC 7086, which are publicly available at the following links:

– https://vizier.cds.unistra.fr/viz-bin/VizieR-3?-source=I/355/gaiadr3 &-out.max=50&-out.form=HTML%20Table&-out.add=_r&-out.add=_RAJ,_DEJ&- sort=_r&-oc.form=sexa
– https://vizier.cds.unistra.fr/viz-bin/VizieR-3?-source=J/A%2bA/6 73/A114&-out.max=50&-out.form=HTML%20Table&-out.add=_Glon,_Glat&- out.add=_RAJ,_DEJ&-oc.form=dec
– https://archive.stsci.edu/cgi-bin/dss_form
– http://stev.oapd.inaf.it/cgi-bin/cmd
– Emily L. Hunt, Private communication, 2024.

References

Adams, F. C. & Myers, P. C., Modes of Multiple Star Formation. 2001, *Astrophysical Journal*, **553**, 744, DOI: 10.1086/320941

Allende Prieto, C., Majewski, S. R., Schiavon, R., et al., APOGEE: The Apache Point Observatory Galactic Evolution Experiment. 2008, *Astronomische Nachrichten*, **329**, 1018, DOI: 10.1002/asna.200811080

Angelo, M. S., Santos, J. F. C., Maia, F. F. S., & Corradi, W. J. B., Investigating Galactic binary cluster candidates with Gaia EDR3. 2022, *Monthly Notices of the RAS*, **510**, 5695, DOI: 10.1093/mnras/stab3807

Balaguer-Núnez, L., Tian, K. P., & Zhao, J. L., Determination of proper motions and membership of the open clusters NGC 1817 and NGC 1807. 1998, *Astronomy and Astrophysics, Supplement*, **133**, 387, DOI: 10.1051/aas:1998324

Baumgardt, H. & Makino, J., Dynamical evolution of star clusters in tidal fields. 2003, *Monthly Notices of the RAS*, **340**, 227, DOI: 10.1046/j.1365-8711.2003.06286.x

Bhatia, R. K. & Hatzidimitriou, D., Binary star clusters in the Large Magellanic Cloud. 1988, *Monthly Notices of the RAS*, **230**, 215, DOI: 10.1093/mnras/230.2215

Binney, J. & Tremaine, S. 2008, *Galactic Dynamics: Second Edition*

Bisht, D., Elsanhoury, W. H., Zhu, Q., et al., An Investigation of Poorly Studied Open Cluster NGC 4337 Using Multicolor Photometric and Gaia DR2 Astrometric Data. 2020, *Astronomical Journal*, **160**, 119, DOI: 10.3847/1538-3881/ab9ffd

Bisht, D., Yadav, R. K. S., & Durgapal, A. K., 2MASS analytical study of four open cluster candidates. 2017, *New Astronomy*, **52**, 55, DOI: 10.1016/j.newast.2016.10.009

Bisht, D., Yadav, R. K. S., Ganesh, S., et al., Mass function and dynamical study of the open clusters Berkeley 24 and Czernik 27 using ground based imaging and Gaia astrometry. 2019, *Monthly Notices of the RAS*, **482**, 1471, DOI: 10.1093/mnras/sty2781

Bland-Hawthorn, J., Sharma, S., Tepper-Garcia, T., et al., The GALAH survey and Gaia DR2: dissecting the stellar disc's phase space by age, action, chemistry, and location. 2019, *Monthly Notices of the RAS*, **486**, 1167, DOI: 10.1093/mnras/stz217

Bonatto, C. & Bica, E., The nature of the young and low-mass open clusters Pismis5, vdB80, NGC1931 and BDSB96. 2009, *Monthly Notices of the RAS*, **397**, 1915, DOI: 10.1111/j.1365-2966.2009.14877.x

Bressan, A., Marigo, P., Girardi, L., et al., PARSEC: stellar tracks and isochrones with the PAdova and TRieste Stellar Evolution Code. 2012, *Monthly Notices of the RAS*, **427**, 127, DOI: 10.1111/j.1365-2966.2012.21948.x

Bukowiecki, L., Maciejewski, G., Konorski, P., & Strobel, A., Open Clusters in 2MASS Photometry. I. Structural and Basic Astrophysical Parameters. 2011, *Acta Astronomica*, **61**, 231, DOI: 10.48550/arXiv.1107.5119

Cantat-Gaudin, T., Jordi, C., Vallenari, A., et al., A Gaia DR2 view of the open cluster population in the Milky Way. 2018, *Astronomy and Astrophysics*, **618**, A93, DOI: 10.1051/0004-6361/201833476

Cardelli, J. A., Clayton, G. C., & Mathis, J. S., The Relationship between Infrared, Optical, and Ultraviolet Extinction. 1989, *Astrophysical Journal*, **345**, 245, DOI: 10.1086/167900

Casagrande, L. & VandenBerg, D. A., On the use of Gaia magnitudes and new tables of bolometric corrections. 2018, *Monthly Notices of the RAS*, **479**, L102, DOI: 10.1093/mnrasl/sly104

Chupina, N. V., Reva, V. G., & Vereshchagin, S. V., The geometry of stellar motions in the nucleus region of the Ursa Major kinematic group. 2001, *Astronomy and Astrophysics*, **371**, 115, DOI: 10.1051/0004-6361:20010337

Chupina, N. V., Reva, V. G., & Vereshchagin, S. V., Kinematic structure of the corona of the Ursa Major flow found using proper motions and radial velocities of single stars. 2006, *Astronomy and Astrophysics*, **451**, 909, DOI: 10.1051/0004-6361:20054009

Conrad, C., Scholz, R. D., Kharchenko, N. V., et al., A RAVE investigation on Galactic open clusters . II. Open cluster pairs, groups and complexes. 2017, *Astronomy and Astrophysics*, **600**, A106, DOI: 10.1051/0004-6361/201630012

de La Fuente Marcos, R. & de La Fuente Marcos, C., Double or binary: on the multiplicity of open star clusters. 2009, *Astronomy and Astrophysics*, **500**, L13, DOI: 10.1051/0004-6361/200912297

De Silva, G. M., Freeman, K. C., Bland-Hawthorn, J., et al., The GALAH survey: scientific motivation. 2015, *Monthly Notices of the RAS*, **449**, 2604, DOI: 10.1093/mnras/stv327

Dias, W. S., Alessi, B. S., Moitinho, A., & Lépine, J. R. D., New catalogue of optically visible open clusters and candidates. 2002, *Astronomy and Astrophysics*, **389**, 871, DOI: 10.1051/0004-6361:20020668

Dib, S. & Basu, S., The emergence of the galactic stellar mass function from a non-universal IMF in clusters. 2018, *Astronomy and Astrophysics*, **614**, A43, DOI: 10.1051/0004-6361/201732490

Dieball, A., Müller, H., & Grebel, E. K., A statistical study of binary and multiple clusters in the LMC. 2002, *Astronomy and Astrophysics*, **391**, 547, DOI: 10.1051/0004-6361:20020815

Durgapal, A. K. & Pandey, A. K., Structure and mass function of five intermediate/old open clusters. 2001, *Astronomy and Astrophysics*, **375**, 840, DOI: 10.1051/0004-6361:20010892

Elsanhoury, W. H., Postnikova, E. S., Chupina, N. V., et al., The Pleiades apex and its kinematical structure. 2018, *Astrophysics and Space Science*, **363**, 58, DOI: 10.1007/s10509-018-3268-3

Evans, D. W., Riello, M., De Angeli, F., et al., Gaia Data Release 2. Photometric content and validation. 2018, *Astronomy and Astrophysics*, **616**, A4, DOI: 10.1051/0004-6361/201832756

Fich, M. & Tremaine, S., The mass of the Galaxy. 1991, *Annual Review of Astron and Astrophys*, **29**, 409, DOI: 10.1146/annurev.aa.29.090191.002205

Fukushige, T. & Heggie, D. C., The time-scale of escape from star clusters. 2000, *Monthly Notices of the RAS*, **318**, 753, DOI: 10.1046/j.1365-8711.2000.03811.x

Gaia Collaboration. 2022, VizieR Online Data Catalog: Gaia DR3 Part 1. Main source (Gaia Collaboration, 2022), VizieR On-line Data Catalog: I/355. Originally published in: Astron. Astrophys., in prep. (2022)

Gaia Collaboration, Brown, A. G. A., Vallenari, A., et al., Gaia Early Data Release 3. Summary of the contents and survey properties. 2021, *Astronomy and Astrophysics*, **649**, A1, DOI: 10.1051/0004-6361/202039657

Gilmore, G., Randich, S., Asplund, M., et al., The Gaia-ESO Public Spectroscopic Survey. 2012, *The Messenger*, **147**, 25

Hassan, S. M., Three-Color Photometry of NGC 7086. 1967, *Zeitschrift fuer Astrophysik*, **66**, 6

Hassan, S. M. & Barbon, R., A photometric study of the open cluster NGC 7031. 1973, *Mem. Societa Astronomica Italiana*, **44**, 39

Hatzidimitriou, D. & Bhatia, R. K., Cluster pairs in the Small Magellanic Cloud. 1990, *Astronomy and Astrophysics*, **230**, 11

Hoag, A. A., Johnson, H. L., Iriarte, B., et al., Photometry of stars in galactic cluster fields. 1961, *Publications of the U.S. Naval Observatory Second Series*, **17**, 344

Hunt, E. L. & Reffert, S., Improving the open cluster census. II. An all-sky cluster catalogue with Gaia DR3. 2023, *Astronomy and Astrophysics*, **673**, A114, DOI: 10.1051/0004-6361/202346285

Hunt, E. L. & Reffert, S., Improving the open cluster census. III. Using cluster masses, radii, and dynamics to create a cleaned open cluster catalogue. 2024, *arXiv e-prints*, arXiv:2403.05143, DOI: 10.48550/arXiv.2403.05143

Inagaki, S. & Saslaw, W. C., Equipartition in multicomponent gravitational systems. 1985, *Astrophysical Journal*, **292**, 339, DOI: 10.1086/163164

Javakhishvili, G., Kukhianidze, V., Todua, M., & Inasaridze, R., A method of open cluster membership determination. 2006, *Astronomy and Astrophysics*, **447**, 915, DOI: 10.1051/0004-6361:20040297

Jeffries, R. D., Thurston, M. R., & Hambly, N. C., Photometry and membership for low mass stars in the young open cluster NGC 2516. 2001, *Astronomy and Astrophysics*, **375**, 863, DOI: 10.1051/0004-6361:20010918

Joshi, Y. C., Dambis, A. K., Pandey, A. K., & Joshi, S., Study of open clusters within 1.8 kpc and understanding the Galactic structure. 2016, *Astronomy and Astrophysics*, **593**, A116, DOI: 10.1051/0004-6361/201628944

Joshi, Y. C., Maurya, J., John, A. A., et al., Photometric, kinematic, and variability study in the young open cluster NGC 1960. 2020, *Monthly Notices of the RAS*, **492**, 3602, DOI: 10.1093/mnras/staa029

Kharchenko, N. V., Piskunov, A. E., Schilbach, E., Röser, S., & Scholz, R. D., Global survey of star clusters in the Milky Way. II. The catalogue of basic parameters. 2013, *Astronomy and Astrophysics*, **558**, A53, DOI: 10.1051/0004-6361/201322302

King, I., The structure of star clusters. I. an empirical density law. 1962, *Astronomical Journal*, **67**, 471, DOI: 10.1086/108756

King, I. R., The structure of star clusters. III. Some simple dynamical models. 1966, *Astronomical Journal*, **71**, 64, DOI: 10.1086/109857

Kopchev, V. S. & Petrov, G. T., BV photometry of a possible open star cluster pair NGC 7031/NGC 7086. 2008, *Astronomische Nachrichten*, **329**, 845, DOI: 10.1002/asna.200711009

Krone-Martins, A. & Moitinho, A., UPMASK: unsupervised photometric membership assignment in stellar clusters. 2014, *Astronomy and Astrophysics*, **561**, A57, DOI: 10.1051/0004-6361/201321143

Küpper, A. H. W., MacLeod, A., & Heggie, D. C., On the structure of tidal tails. 2008, *Monthly Notices of the RAS*, **387**, 1248, DOI: 10.1111/j.1365-2966.2008.13323.x

Lada, C. J. & Lada, E. A., Embedded Clusters in Molecular Clouds. 2003, *Annual Review of Astron and Astrophys*, **41**, 57, DOI: 10.1146/annurev.astro.41.011802.094844

Lindoff, U., The ages of open clusters. 1968, *Arkiv for Astronomi*, **5**, 1

Liu, J. C., Zhu, Z., & Hu, B., Constructing a Galactic coordinate system based on near-infrared and radio catalogs. 2011, *Astronomy and Astrophysics*, **536**, A102, DOI: 10.1051/0004-6361/201116947

Netopil, M., Paunzen, E., & Stütz, C., Developments of the Open Cluster Database WEBDA. 2012, in Astrophysics and Space Science Proceedings, Vol. **29**, *Star Clusters in the Era of Large Surveys*, 53

Perren, G. I., Giorgi, E. E., Moitinho, A., et al., Sixteen overlooked open clusters in the fourth Galactic quadrant. A combined analysis of UBVI photometry and Gaia DR2 with ASteCA. 2020, *Astronomy and Astrophysics*, **637**, A95, DOI: 10.1051/0004-6361/201937141

Perren, G. I., Vázquez, R. A., & Piatti, A. E., ASteCA: Automated Stellar Cluster Analysis. 2015, *Astronomy and Astrophysics*, **576**, A6, DOI: 10.1051/0004-6361/201424946

Phelps, R. L. & Janes, K. A., Young Open Clusters as Probes of the Star-Formation Process. II. Mass and Luminosity Functions of Young Open Clusters. 1993, *Astronomical Journal*, **106**, 1870, DOI: 10.1086/116772

Piatti, A. E., A comprehensive photometric study of dynamically evolved small van den Bergh-Hagen open clusters. 2016, *Monthly Notices of the RAS*, **463**, 3476, DOI: 10.1093/mnras/stw2248

Piatti, A. E., Bica, E., Santos, J. F. C., J., & Clariá, J. J., A revision of the fundamental parameters of the open cluster Hogg 15 and the projected star WR 47. 2002, *Astronomy and Astrophysics*, **387**, 108, DOI: 10.1051/0004-6361:20020373

Pietrzynski, G. & Udalski, A., The Optical Gravitational Lensing Experiment. Multiple Cluster Candidates in the Large Magellanic Cloud. 2000, *Acta Astronomica*, **50**, 355, DOI: 10.48550/arXiv.astro-ph/0010294

Piskunov, A. E., Belikov, A. N., Kharchenko, N. V., Sagar, R., & Subramaniam, A., On the determination of age and mass functions of stars in young open star clusters from the analysis of their luminosity functions. 2004, *Monthly Notices of the RAS*, **349**, 1449, DOI: 10.1111/j.1365-2966.2004.07620.x

Rangwal, G., Yadav, R. K. S., Durgapal, A., Bisht, D., & Nardiello, D., Astrometric and photometric study of NGC 6067, NGC 2506, and IC 4651 open clusters based on wide-field ground and Gaia DR2 data. 2019, *Monthly Notices of the RAS*, **490**, 1383, DOI: 10.1093/mnras/stz2642

Rosvick, J. M. & Robb, R., A Photometric Search for Planets in the Open Cluster NGC 7086. 2006, *Astronomical Journal*, **132**, 2309, DOI: 10.1086/508517

Salpeter, E. E., The Luminosity Function and Stellar Evolution. 1955, *Astrophysical Journal*, **121**, 161, DOI: 10.1086/145971

Santos-Silva, T. & Gregorio-Hetem, J., Characterisation of young stellar clusters. 2012, *Astronomy and Astrophysics*, **547**, A107, DOI: 10.1051/0004-6361/201219695

Scalo, J., The IMF Revisited: A Case for Variations. 1998, in Astronomical Society of the Pacific Conference Series, Vol. **142**, *The Stellar Initial Mass Function (38th Herstmonceux Conference)*, ed. G. Gilmore & D. Howell, 201

Scott, D. W. 1992, *Multivariate Density Estimation*

Spitzer, Lyman, J. & Hart, M. H., Random Gravitational Encounters and the Evolution of Spherical Systems. I. Method. 1971, *Astrophysical Journal*, **164**, 399, DOI: 10.1086/150855

Subramaniam, A., Gorti, U., Sagar, R., & Bhatt, H. C., Probable binary open star clusters in the Galaxy. 1995, *Astronomy and Astrophysics*, **302**, 86

Sung, H. & Bessell, M. S., The Initial Mass Function and Stellar Content of NGC 3603. 2004, *Astronomical Journal*, **127**, 1014, DOI: 10.1086/381297

Svolopoulos, S. N., Spectral Classification in Some Open Clusters. 1961, *Astrophysical Journal*, **134**, 612, DOI: 10.1086/147183

von Hoerner, S., Internal structure of globular clusters. 1957, *Astrophysical Journal*, **125**, 451, DOI: 10.1086/146321

Šablevičiūtė, I., Vansevičius, V., Kodaira, K., et al., A Survey of Compact Star Clusters in the South-West Field of the M 31 Disk. Structural Parameters. 2006, *Baltic Astronomy*, **15**, 547, DOI: 10.48550/arXiv.astro-ph/0701774

Yadav, R. K. S. & Sagar, R., A deep UBVRI CCD photometric study of the open clusters Tr1 and Be 11. 2002, *Monthly Notices of the RAS*, **337**, 133, DOI: 10.1046/j.1365-8711.2002.05888.x

Yadav, R. K. S. & Sagar, R., UBVRI CCDphotometric studyoftheopen clusters Basel 4 and NGC 7067. 2004, *Monthly Notices of the RAS*, **349**, 1481, DOI: 10.1111/j.1365-2966.2004.07623.x

Yadav, R. K. S., Sariya, D. P., & Sagar, R., Proper motions and membership probabilities of stars in the region of open cluster NGC 3766. 2013, *Monthly Notices of the RAS*, **430**, 3350, DOI: 10.1093/mnras/stt136

Yontan, T., Bilir, S., Bostancı, Z. F., et al., CCD UBV photometric and Gaia astrometric study of eight open clusters—ASCC 115, Collinder 421, NGC 6793, NGC 7031, NGC 7039, NGC 7086, Roslund 1 and Stock 21. 2019, *Astrophysics and Space Science*, **364**, 152, DOI: 10.1007/s10509-019-3640-y

Zeidler, P., Nota, A., Grebel, E. K., et al., A High-resolution Multiband Survey of Westerlund 2 with the Hubble Space Telescope. III. The Present-day Stellar Mass Function. 2017, *Astronomical Journal*, **153**, 122, DOI: 10.3847/1538-3881/153/3/122

Zhong, J., Chen, L., Kouwenhoven, M. B. N., et al., Substructure and halo population of Double Cluster h and χ Persei. 2019, *Astronomy and Astrophysics*, **624**, A34, DOI: 10.1051/0004-6361/201834334